Progress In Electromagnetics Research, PIER 92, 299–315, 2009

REALIZATION OF COMPOSITE RIGHT/LEFT-HANDED TRANSMISSION LINE USING COUPLED LINES

A. F. Abdelaziz, T. M. Abuelfadl, and O. L. Elsayed

Department of Electronics and Electrical Engineering
Cairo University
12613, Egypt

Abstract—This paper presents a method to construct composite right/left-handed transmission line using coupled lines. A general procedure to design a composite right/left-handed unit cell is presented. The procedure was used on a specific coupled line configuration, which is the coupled microstrip lines with slotted ground. It is shown that by proper design of the slotted ground, the coupling between the two microstrip lines can be increased dramatically keeping practical dimensions for the coupled line width and spacing. Moreover, with accurate slotted ground design, equal even and odd electrical lengths can be achieved. The performance of this composite right/left-handed line, which is characterized by backward waves with phase advance, is demonstrated by both simulated and measured results and they show good agreement. The realized composite right/left-handed transmission line has a broad bandwidth and small size.

1. INTRODUCTION

The conventional transmission line (right-handed TL) is represented by a series inductor and a shunt capacitance, implying the use of a low pass topology. By interchanging the position of the inductor and capacitor, the resulting structure is referred to as left-handed transmission line with a high pass configuration. The homogeneous models of a purely right-handed and purely left-handed lossless transmission line are shown in Fig. 1. In this left-handed lines, the phase and group velocities are opposite to each other. The left-handed transmission line is sometimes considered as the 1-D version of the so called

Corresponding author: A. F. Abdelaziz (ayafekry@yahoo.com).

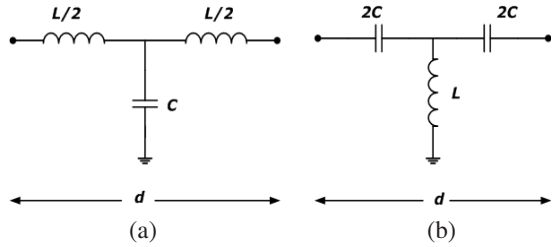

Figure 1. (a) RH TL. (b) LH TL.

metamaterials [1]. Composite right/left-handed (CRLH) transmission lines represent practical left-handed TL, because right-handed parasitic effects are unavoidable when the realization of a left-handed TL is attempted. A 1-D CRLH transmission line was designed before in the form of an ideal lumped-elements ladder network, and then a microstrip implementation of the CRLH TL, using interdigital capacitors and stub inductors, was realized [1].

We present here a transmission line approach of CRLH materials based on using coupled lines. In principle, the line can be implemented using any type of coupled transmission line. However, as will be shown later, the required coupling and the available technology impose limitations on manufacturing. In this paper, the CRLH transmission line is implemented using edge coupled microstrip lines with ground plane aperture on the FR-4 board as shown in Fig. 2(b). High coupling can not achieved in conventional edge coupled microstrip lines unless the interline spacing is very small which is impractical. The floating aperture makes it possible to design CRLH transmission line while maintaining all connections in the same plane and in the same time increases the coupling [2, 3]. The CRLH transmission line is fabricated and measured. Experimental and simulated data are compared to each other.

The paper is organized as follows: Section 2 presents the unit cell approach of CRLH structures with a pair of coupled lines which can be connected in two different configurations. This is considered a general procedure to design CRLH transmission line using coupled lines. The unit cell dispersion and Bloch impedance are analyzed and demonstrated. In Section 3, we focus on our specific realization of the coupled lines using coupled microstrip lines with slotted ground, the reason for using the slotted ground is explained, and the implementation of the CRLH transmission line is shown together with the simulation results for the dispersion diagram. In Section 4, a comparison between the measurement and the simulation of the CRLH design is demonstrated. Finally, conclusions are given in Section 5.

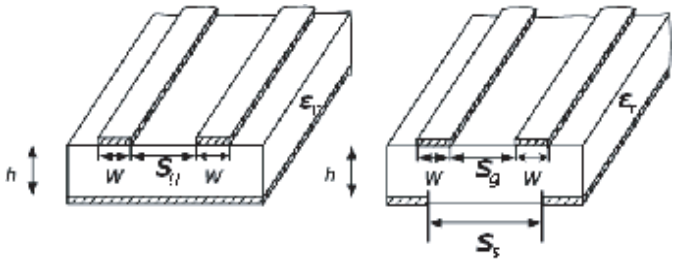

(a) (b)

Figure 2. Coupled microstrip lines. (a) Edge coupled. (b) Edge coupled microstrip lines with floating strip in the ground plane.

2. UNIT COMPOSITE RIGHT/LEFT HAND CELL

2.1. Coupled Lines

Symmetric coupled lines operation can be described in terms of the even and odd modes [4]. These even and odd modes are characterized by the characteristic impedance and electrical length, denoted respectively as (Z_{oe}, θ_e) and (Z_{oo}, θ_o), where the letters e and o denote the even and odd parameters, respectively. The dielectric medium for the coupled microstrip lines is not homogeneous, resulting in different propagation velocities for the even and odd modes. However, in our present design, adding the floating slot in the ground conductor as shown in Fig. 2(b) tends to equalize the even and the odd phase velocities. As a result, the coupling between the two microstrip lines will be described using homogeneous dielectric medium equations [4], where the coupled lines electrical lengths are the same for both the even and odd modes ($\theta_e = \theta_o = \theta$). Homogeneous symmetrical coupled lines, schematically shown in Fig. 3 as a four-port network, can be described by the impedance matrix $[Z]$. Voltages and currents on the four ports in Fig. 3 are related by, $[V] = [Z][I]$. The sixteen elements of the impedance matrix $[Z]$ are given as [4],

$$\begin{aligned}
Z_{11} = Z_{22} = Z_{33} = Z_{44} &= -j(Z_{oe} + Z_{oo})\frac{\cot\theta}{2} \\
Z_{12} = Z_{21} = Z_{34} = Z_{43} &= -j(Z_{oe} - Z_{oo})\frac{\cot\theta}{2} \\
Z_{13} = Z_{31} = Z_{24} = Z_{42} &= -j(Z_{oe} - Z_{oo})\frac{\csc\theta}{2} \\
Z_{14} = Z_{41} = Z_{23} = Z_{32} &= -j(Z_{oe} + Z_{oo})\frac{\csc\theta}{2}.
\end{aligned} \tag{1}$$

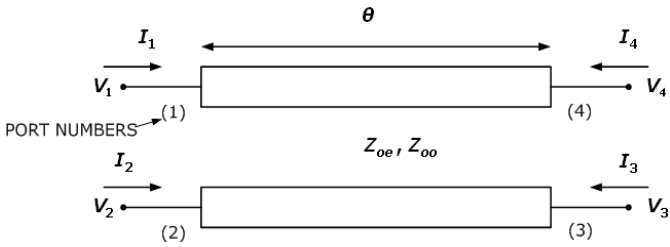

Figure 3. Schematic of pair of coupled lines.

Now, the unit cell can be achieved using the following steps. We terminate port 3 and port 4 with short and open circuits, respectively. This results in $V_3 = 0$ and $I_4 = 0$, and the network becomes a two-port network. Hence (1) becomes,

$$\begin{aligned} V_1 &= Z_{11}I_1 + Z_{12}I_2 + Z_{13}I_3 \\ V_2 &= Z_{12}I_1 + Z_{11}I_2 + Z_{14}I_3 \\ 0 &= Z_{13}I_1 + Z_{14}I_2 + Z_{11}I_3. \end{aligned} \tag{2}$$

Eliminating I_3 from these equations, it is found that

$$\begin{aligned} V_1 &= \left(Z_{11} - \frac{Z_{13}^2}{Z_{11}}\right) I_1 + \left(Z_{12} - \frac{Z_{14}Z_{13}}{Z_{11}}\right) I_2 \\ V_2 &= \left(Z_{12} - \frac{Z_{13}Z_{14}}{Z_{11}}\right) I_1 + \left(Z_{11} - \frac{Z_{14}^2}{Z_{11}}\right) I_2. \end{aligned} \tag{3}$$

The above equation can be rearranged to get the $ABCD$ transmission matrix description of this network as

$$\begin{pmatrix} A & B \\ C & D \end{pmatrix} = \begin{pmatrix} \frac{Z_{oe}-Z_{oo}}{Z_{oe}+Z_{oo}}\left(1 - \frac{4Z_{oe}Z_{oo}\cot^2\theta}{(Z_{oe}-Z_{oo})^2}\right) & \frac{-2jZ_{oe}Z_{oo}\cot\theta}{Z_{oe}-Z_{oo}} \\ \frac{-2j\cot\theta}{Z_{oe}-Z_{oo}} & \frac{Z_{oe}+Z_{oo}}{Z_{oe}-Z_{oo}} \end{pmatrix} \tag{4}$$

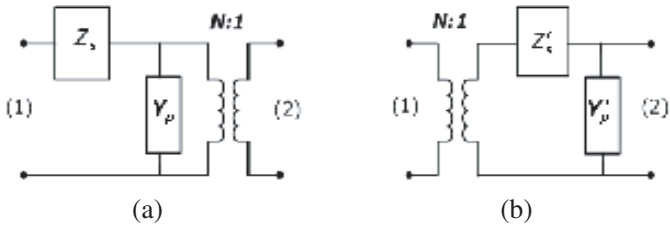

(a) (b)

Figure 4. (a) Realization 1. (b) Realization 2.

It is clear from the $ABCD$ transmission matrix given by (4) that the circuit can be represented as a cascaded network composed of an ideal transformer, a series impedance and a parallel admittance. Equation (4) can be represented by either two configurations depending on the transformer position. Fig. 4 shows the two circuit representations which are equivalent to the original circuit. The equivalent circuit parameters in Fig. 4 are given by,

$$\begin{aligned} Z_s &= \frac{1}{j\omega C_s} = \frac{-2jZ_{oo}Z_{oe}\cot\theta}{Z_{oe}+Z_{oo}} \\ Y_p &= \frac{1}{j\omega L_p} = \frac{-2j(Z_{oo}+Z_{oe})\cot\theta}{(Z_{oe}-Z_{oo})^2} \\ N &= \frac{Z_{oe}-Z_{oo}}{Z_{oe}+Z_{oo}} \qquad Z_s' = N^2 Z_s \qquad Y_p' = Y_p/N^2 \end{aligned} \tag{5}$$

The series impedances Z_s and Z_s' act as capacitive reactance for frequencies corresponding to coupled lines electrical length $\theta < \pi/2$, and become inductive for $\theta > \pi/2$. Similarly the parallel admittances Y_p and Y_p' are inductive susceptance for $\theta < \pi/2$ and capacitive for $\theta > \pi/2$.

Finally, the composite right/left hand unit cell can be constructed by cascading the circuit with its mirrored version (back-to-back

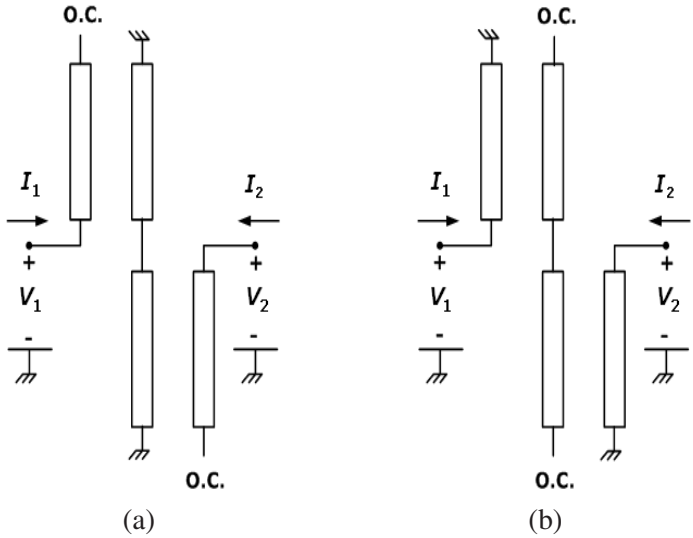

Figure 5. (a) OSO Coupled line. (b) SOS Coupled line.

connection) to cancel the presence of the ideal transformer. From left to right, if we take the first part of the unit cell from the circuit and cascade it with its mirror, we end up with the unit cell shown in Fig. 5(a). Its equivalent circuit is shown in Fig. 6. This equivalent circuit is obtained by cascading the circuit configuration shown in Fig. 4(a) with its mirror, the ideal transformers cancel each other and we end up with the T-network shown. However, if we reverse the order of the two parts, we get the circuit shown in Fig. 5(b). Its equivalent circuit is shown in Fig. 7. This equivalent circuit is obtained by cascading the circuit configuration shown in Fig. 4(b) with its mirror and gives the Π network shown. We will call the configuration in Fig. 5(a) OSO, denoting that the two sides are open circuited lines coupled to the middle connected short circuited lines. Similarly, we will call the configuration of Fig. 5(b) SOS.

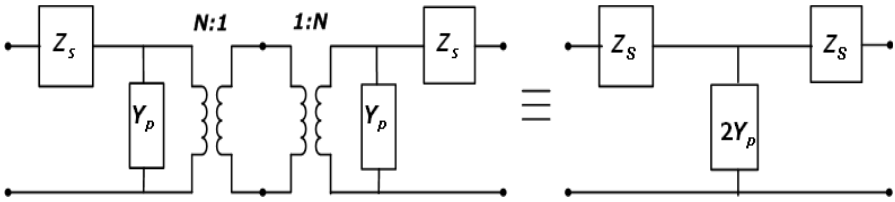

Figure 6. Realization of the cascaded OSO configuration.

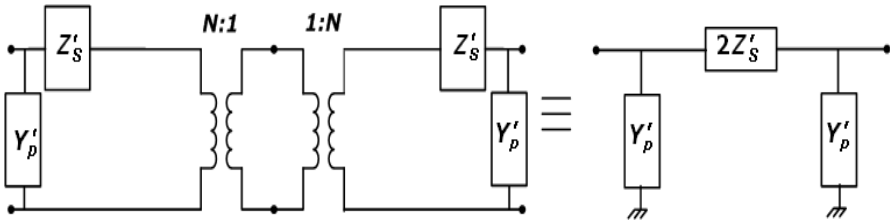

Figure 7. Realization of the cascaded SOS configuration.

2.2. Floquet Analysis and Design of Unit Cell

The equivalent circuits shown in Fig. 6 and Fig. 7 can be seen as lumped elements capacitors and inductors if we introduce the Richard frequency $\Omega = \tan\theta$, which now plays the rule of ω in lumped circuits. This transformation is commonly referred to as the Richard transformation [5].

The T and Π networks, Fig. 7 and Fig. 8, respectively, act as left-handed cells to build a left-handed transmission line for the range of frequency $\theta < \pi/2$. The line becomes right-handed with the equivalent circuit of series inductor and parallel capacitor for $\theta > \pi/2$. In that sense the synthetic line constructed from either one of the two unit cells in Figs. 6 and 7 can be called composite right-left handed (CRLH).

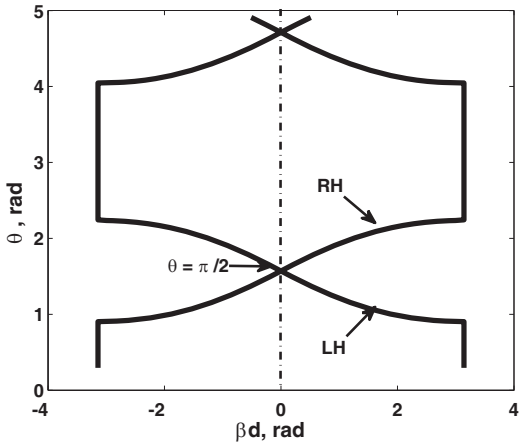

(a) Dispersion diagram.

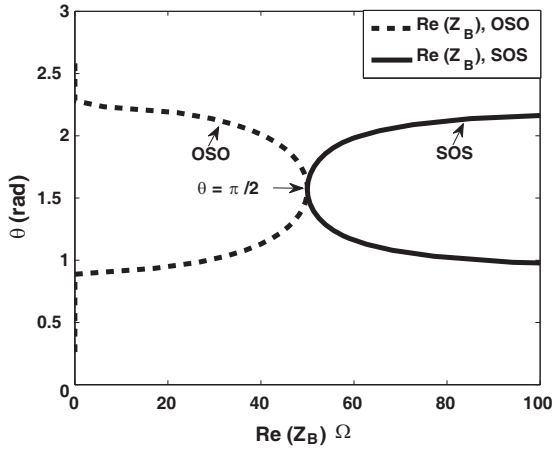

(b) Bloch impedance Z_B

Figure 8. The main parameters of a periodic structure calculated with $Z_{oe} = 184.46\,\Omega$ and $Z_{oo} = 73.78\,\Omega$.

The structure obtained through cascading either the OSO or the SOS configurations is a periodic structure and can be analyzed using the Floquet theorem [6]. Floquet theorem gives the propagation factor β and Bloch impedance Z_B by [7]

$$\cos \beta d = 1 + \frac{Z_s Y_p}{2} = 1 + \frac{Z'_s Y'_p}{2} \tag{6}$$

$$Z_B = \begin{cases} \frac{\sqrt{(Z_s Y_p)^2 + Z_s Y_p}}{Y_p} & \text{OSO configuration} \\ \frac{\sqrt{Z'_s}}{\sqrt{Y'_p(1+Z'_s Y'_p)}} & \text{SOS configuration} \end{cases} \tag{7}$$

where d the unit cell length. The unit cell phase shift of βd is the one defined by the dispersion Equation (6), where β is obtained after dividing by the cell physical length d. The periodic structure dispersion is obtained by plotting the θ-βd relation where θ is taken as a normalization for the frequency ω (with a linear relation between θ and ω), and βd, the phase shift along one cell, is the normalization to the propagation factor β. Fig. 8(a) shows this dispersion relation with passbands and stopbands of the periodic structure. The passband regions are those for which the propagation βd is pure real; in other words $|\cos(\beta d)| \leq 1$. Using this condition and the dispersion Equation (6) after substituting with Z_s and Y_p from Equation (5) the first passband occurs within the θ range given by,

$$\begin{aligned} &\pi/2 - \sin^{-1}[(Z_{oe} - Z_{oo})/(Z_{oe} + Z_{oo})] < \theta \\ &< \pi/2 + \sin^{-1}[(Z_{oe} - Z_{oo})/(Z_{oe} + Z_{oo})] \end{aligned} \tag{8}$$

In Fig. 8(a), it is clear that inside the first pass band for $\theta < \pi/2$ the propagating mode is a backward mode or a left-handed mode and becomes forward or right-handed for $\theta > \pi/2$. The passband region width increases with the increase of the ratio between the even and odd impedance Z_{oe}/Z_{oo}; in other words, the bandwidth of both the left-handed and the right-handed regions increase as the lines become tightly coupled.

In the pass band region the Bloch impedance (7) is pure real value. A comparison of the Bloch impedance for the OSO and SOS configurations is shown in Fig. 8(b). The design for a a composite right/left handed transmission line requires terminating the line with its Bloch impedance for proper matching. The Bloch impedance is a frequency dependent function. However, for a small frequency range of interest it can be considered as constant. The minimum variation of Z_B with frequency is near $\theta = \pi/2$. Although the line characteristic impedance can be designed for any desired frequency, we will choose

the extreme point $\theta = \pi/2$ in our design for simplicity. So at $\theta = \pi/2$, Z_B is chosen as equal to our matching terminating impedance Z_o (i.e., $Z_o = 50\,\Omega$). Hence from [7], the design equations for the SOS and OSO

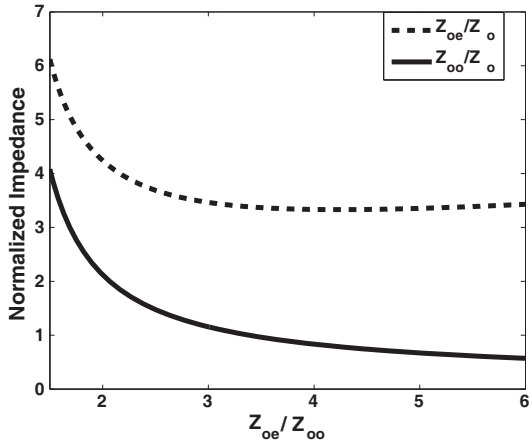

(a) Z_{oe} and Z_{oo} for the OSO.

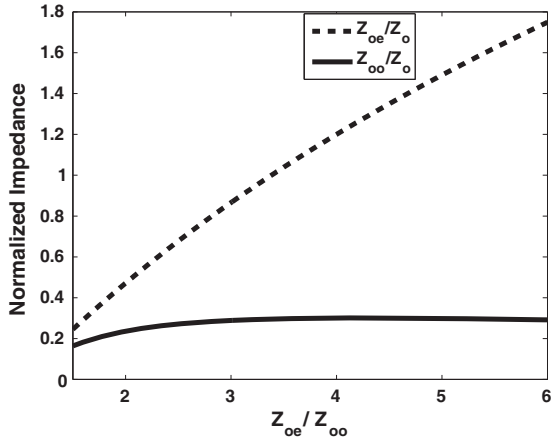

(b) Z_{oe} and Z_{oo} for the SOS.

Figure 9. Dependence of Z_{oe} and Z_{oo} on their ratio.

become,

$$Z_o^2 = Z_{oe}Z_{oo}\left(\frac{Z_{oe}-Z_{oo}}{Z_{oe}+Z_{oo}}\right)^2, \qquad \text{OSO configuration} \tag{9}$$

$$Z_o^2 = Z_{oe}Z_{oo}\left(\frac{Z_{oe}+Z_{oo}}{Z_{oe}-Z_{oo}}\right)^2, \qquad \text{SOS configuration} \tag{10}$$

Figure 9 shows the dependence of the even and odd impedances on the ratio of Z_{oe} and Z_{oo}. The choice of the suitable configuration depends on the method of implementation. For an implementation that can realize large Z_{oe} and Z_{oo} relative to Z_o, the OSO is a proper choice, but for low impedance values SOS is the proper choice. Besides the configuration method, the technology available determines how much bigger Z_{oe}/Z_{oo} can be realized. As mentioned before, the bigger the ratio of Z_{oe}/Z_{oo} the wider the bandwidth of the line under consideration. In the next section, a theoretical design and implementation of a CRLH transmission line using the OSO configuration is presented. The CRLH transmission line is implemented using coupled microstrip lines with slotted ground. The OSO configuration is chosen as it provides large values of Z_{oe} and Z_{oo} which is suitable for our new design.

3. IMPLEMENTATION

The normalized even and odd impedances for both the OSO and the SOS lines configurations are shown in Fig. 9. Choosing the operating point (Z_{oe} and Z_{oo}) depends on the method of implementing the coupled lines and the available technology.

The large difference between the values of Z_{oe} and Z_{oo} is an obstacle in realizing this coupled line by the conventional designs which uses edge coupled microstrip. Coupled microstrip lines have great advantages as they use only a single dielectric substrate and hence they are easy in fabrication, beside they are the most popular for realizing microwave integrated circuits. However, using the coupled microstrip lines imposes some limitations on the design as they have weak coupling. In this paper, we try to implement the unit cell of the CRLH transmission line using coupled microstrip lines but with floating ground. The structure composed of coupled microstrip lines with floating slot has already been analyzed theoretically and experimentally using full wave analysis [2]. The floating slot at the ground plane solves the difficulties arising in the design procedure and the fabrication process as it relaxes the requirements on physical dimensions of the lines. Introducing the floating slot increase the

coupling dramatically by increasing the capacitive coupling, while maintaining all connections at the same plane. The coupling factor rises rapidly as the aperture is widened. Moreover, the floating slot equalizes the even and odd phase velocities as part of the electric field lines in the even excitation extends in air as in the odd excitation, as shown in Fig. 10. This means that Z_{oo} remains nearly the same while Z_{oe} increases. We design first for the required value of Z_{oo} without the slot, then the design is refined and optimized using EM Ansoft designer.

In the present design, a substrate FR-4 with dielectric constant

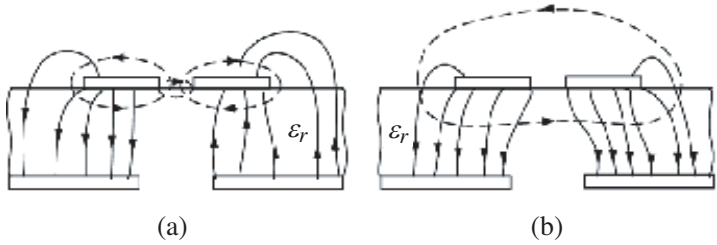

Figure 10. Electric field lines. (a) Odd excitation. (b) Even excitation.

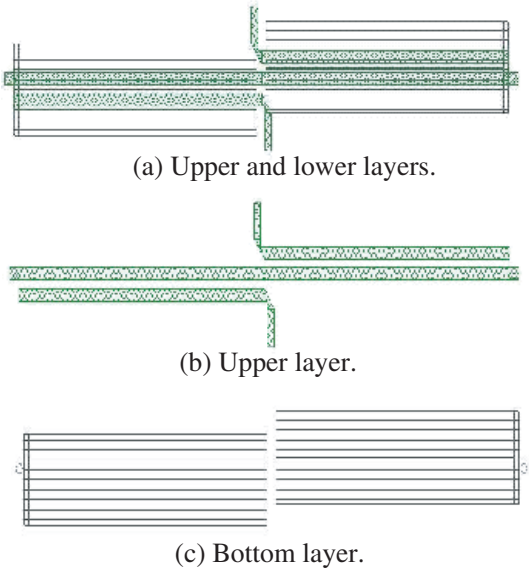

Figure 11. A layout of a unit cell of the novel CRLH TL.

$\varepsilon_r = 4.4$ and thickness $h = 1.6\,\text{mm}$ (loss tangent = 0.02) has been used. The gap between the two coupled lines S_g is designed to be as small as is easily realizable. To realize $Z_{oe} = 184.46\,\Omega$ and $Z_{oo} = 73.78\,\Omega$ taken from Fig. 9, the values of W, S_g and S_s, as shown in Fig. 2, should be 0.68 mm, 0.5 mm, and 5 mm; respectively. The port hight and width are 4 mm and 2.89 mm; respectively. Fig. 11 shows the unit cell of the designed CRLH transmission line circuit. Fig. 11(a) shows the layout of the unit cell with the upper and the lower layers above each other. Fig. 11(b) shows the layout of the top layer, the shaded area represents the coupled microstrip lines. While Fig. 11(c) shows the layout of the ground plane, the shaded area represents the floating slot (no metallization). The small holes are vias added between the

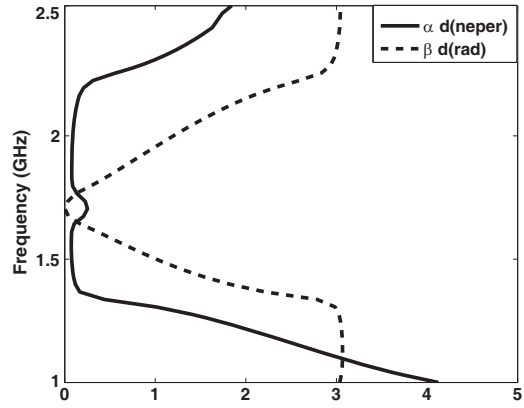

(a) The dispersion diagram.

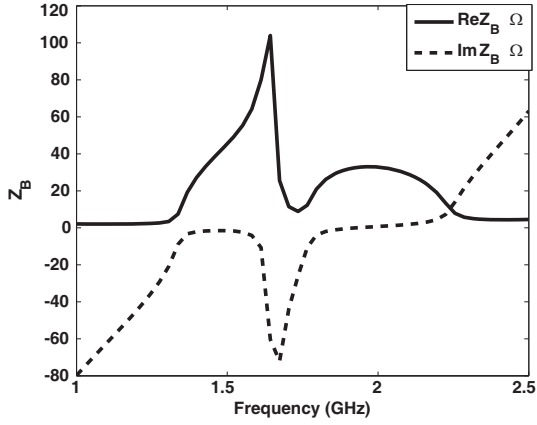

(b) The Bloch impedance.

Figure 12. The performance of the LH cell.

upper and the lower ground conductors to keep them at the same ground potential and to avoid exciting the parallel plate waveguide modes between these conductors. The length of the coupled lines of a unit cell is 26 mm, the length of the slot is 25.5 mm, and the length of the unit cell itself is 6 mm (i.e., the unit cell is repeated periodically every 6 mm).

For our symmetrical T unit cell with Z-parameters Z_{11} and Z_{12}, the dispersion and the Bloch impedance of the unit cell are [6]

$$\cosh \gamma d = \frac{Z_{11}}{Z_{12}} \qquad Z_B = Z_{12} \sinh \gamma d \tag{11}$$

where the Z-parameters were obtained using the method of moments by the EM Ansoft Designer.

Transmission line junctions were added between the coupled lines to prevent overlapping between cells. Although our design goal was to achieve balanced CRLH transmission line, the added TL junctions deform the balanced characteristic and a small band-gap appears between the left-handed and right-handed transmission bands, as shown in Fig. 12(a). This deformation is more pronounced in the Bloch impedance characteristic as it has an imaginary value during the transmission band, shown in Fig. 12(b). In that figure, the matched point $Z_o = 50\,\Omega$ is at 1.6 GHz. Fig. 12(a) indicates attenuation αd of about 0.07 Np, which is due to the dielectric losses in FR-4. material used, but this was greatly reduced in the simulation when the loss tangent of the dielectric material was set to zero.

For our design, we used 5 cells to realize the CRLH TL, this number provides acceptable attenuation. The length of the whole structure is 35 mm. Fig. 13 represents the layout of the proposed CRLH transmission line.

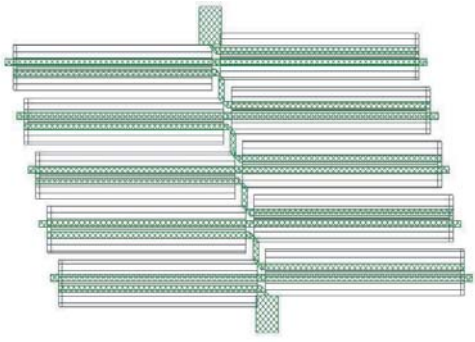

Figure 13. Layout of 5 unit cells OSO configuration CRLH TL.

The proposed CRLH transmission line has been fabricated, measured and compared to the simulation results. A photograph of the proposed CRLH transmission line is shown in Fig. 14.

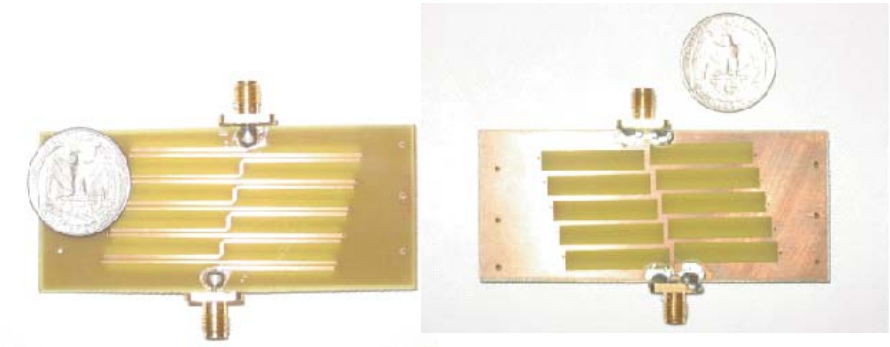

(a) Photograph of the top layer. (b) Photograph of the bottom layer.

Figure 14. Photograph of the proposed CRLH transmission line.

4. MEASUREMENT RESULTS

The S-parameters of the 5 cell transmission line are measured using vector network analyzer. The simulation and the measurements are shown in Fig. 15. This figure shows relatively high losses in the passband around 2.4 dB. This is mostly attributed to the large

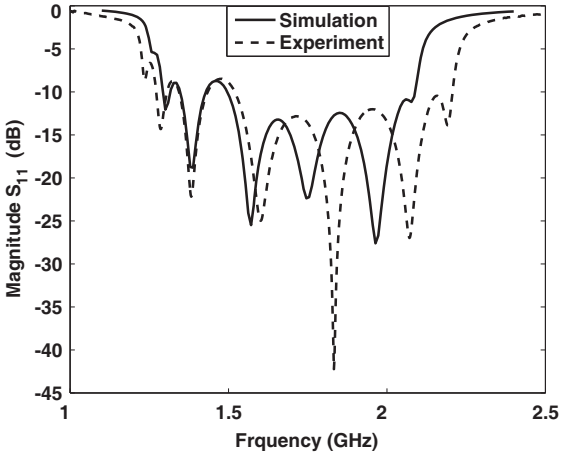

(a) Magnitude of $S_{11,N}$.

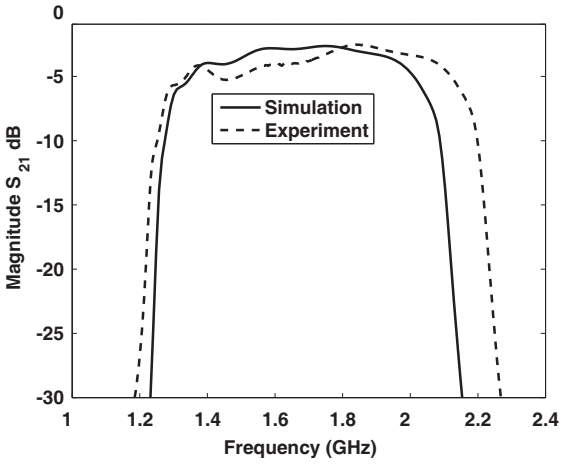

(b) Magnitude of $S_{21,N}$.

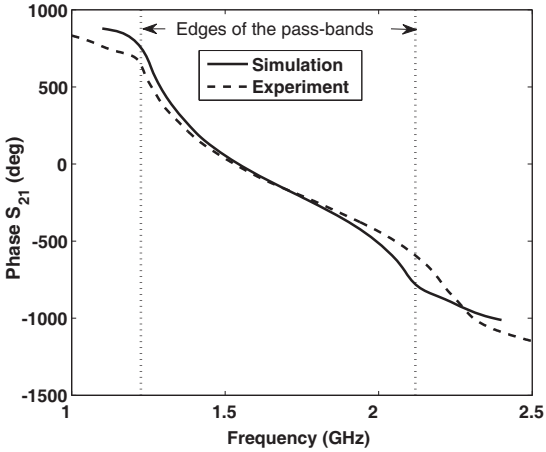

(c) Unwrapped phase.

Figure 15. Frequency characteristics of the CRLH TL.

dielectric losses in FR-4 material. These losses disappear in the simulation when we set the dielectric loss tangent to zero. That means that when using material other than FR-4 with lower loss tangent, the transmission characteristics of the proposed CRLH transmission line are improved. Discrepancies between simulated and measured results probably come from connectors discontinuities and measuring errors, as the simulation results have shown low sensitivity to the variation of the unit cell parameters. Fig. 15(c) shows the unwrapped phase of

$S_{21,N}$. That phase unwrapping is performed around 1.54 GHz for both the simulation and the experiment. The non-linearity of the (φ, ω) curve, as shown in Fig. 15(c), is clear near the edges of the passbands, which is a characteristic of the CRLH TL's.

Because the characteristic impedance is a function of frequency, in general the CRLH transmission line can only be matched in a restricted frequency band. The CRLH networks exhibit band-pass filters performance. From Figs. 15(a) and (b), the 5 cell transmission line acts as a bandpass filter between 1.25 GHz and 2 GHz.

5. CONCLUSION

A CRLH transmission line, depending on the electromagnetic coupling between a pair of coupled lines, has been proposed. The coupling between the lines and its effect has been studied and has led to the design of the unit CRLH cell. The transmission characteristics ($\omega - \beta$ diagram, Bloch impedance) of the proposed CRLH unit cell have been given and interpreted. The presented procedure is general and can be implemented on different coupled lines configurations depending on the available technology. We verified this idea through implementation on coupled microstrip lines with slotted ground. The configuration was used to achieve the large difference between the values of the even and odd impedances of the coupled lines by increasing the capacitive coupling and in the same time compensate for the unequal modal electrical length. Finally, an implementation for the CRLH transmission line has been done and measured and showed a good agreement with the simulated results.

This new CRLH transmission line can be used in many applications such as guided wave applications, as zeroth order resonator and dual band components, due to the great properties of the CRLH TL. One of its possible applications is the use of this structure as a leaky wave antenna. This will be the subject for a future study. Our implementation has similarity with other distributed elements implementation of CRLH [1], such as narrow bandwidth and ease of fabrication compared with lumped element realizations. However, it has the unique advantage of its smaller cell size compared with the other implementation. This small size arises from that our distributed elements (coupled lines) are in the lateral dimension so we can save space and realize smaller lines with more homogeneous criteria (cell size much smaller than wavelength).

REFERENCES

1. Caloz, C. and T. Itoh, "Transmission line approach of left handed LH materials and microstrip impelementation of an artificial LH transmission line," *IEEE Transactions on Antennas and Propagation*, Vol. 52, 1159–1166, May 2004.
2. Masot, F., F. Medina, and M. Horno, "Theoretical and experimental study of modified coupled strip coupler," *Electron. Lett.*, Vol. 28, No. 4, 347–348, Feb. 1992.
3. Velazquez-Ahumada, M., J. Martel, and F. Medina, "Parallel coupled microstrip filters with ground-plane aperature for spurious band suppression and enhanced coupling," *IEEE Transactions on Microwave Theory and Techniques*, Vol. 52, No. 3, 1082–1086, Mar. 2004.
4. Jones, E. M. T. and J. T. Bolljahn, "Coupled-strip-transmission-line filters and directional couplers," *IRE Transactions on Microwave Theory and Techniques*, 75–81, Apr. 1956.
5. Richard, P. I., "Resistor-transmission line circuits," *IRE Transactions on Microwave Theory and Techniques*, Vol. 36, 217–230, Feb. 1948.
6. Pozar, D. M., *Microwave Engineering*, John Wiley and Sons, 1998.
7. Caloz, C. and T. Itoh, *Electromagnetic Metamaterials: Transmission Line Theory and Microwave Applications*, John Wiley & Sons, 2006.